

BEAM-BEAM INTERACTION FOR TILTED STORAGE RINGS*

D. Xu[†], Y. Luo, D. Holmes, C. Montag, F. Willeke, Brookhaven National Laboratory, Upton, NY, USA
Y. Hao, Michigan State University, East Lansing, MI, USA
J. Qiang, Lawrence Berkeley National Laboratory, Berkeley, CA, USA

Abstract

In the Electron-Ion Collider (EIC) design, to avoid vertical orbit bumps in the Electron Storage Ring (ESR) at some crossing points with Hadron Storage Ring (HSR) to preserve the electron polarization, we plan to tilt the ESR plane by $200 \mu\text{rad}$ with an axis connecting IP6 and IP8. In this article, we study the beam-beam interaction when two rings are not in the same plane. The Lorentz boost formula is derived and the required vertical crabbing strength is calculated to compensate the dynamic effect. The beam-beam simulations are performed to validate the theory.

INTRODUCTION

A large crossing angle in the interaction region (IR) is necessary for fast separation of two colliding beams in ring-type colliders to achieve high collision rates, IR background minimization, and overall detector component and IR magnet arrangements. Crab crossing is an effective way to restore the head-on collision for circular colliders [1]. The crab crossing scheme was first successfully implemented at KEKB-factory [2]. The crab cavities, which are key components in the crab crossing scheme, were also demonstrated for the hadron beam in CERN's Super Proton Synchrotron (SPS) recently [3]. Other dynamics effects about the crab cavities can be found in [4–6].

The Electron-Ion Collider (EIC) project adopts the local scheme to achieve the desired luminosity $10^{34} \text{ cm}^{-2}\text{s}^{-1}$ [7], as shown in Fig. 1. In the local scheme, a pair of crab

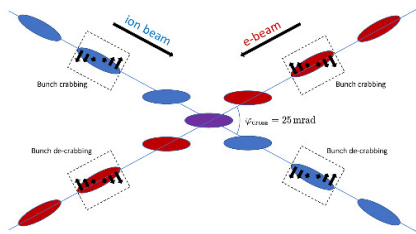


Figure 1: EIC local crabbing compensation scheme [7].

cavities are installed at both sides of the interaction point (IP). The upstream crab cavity tilts the beam in $x-z$ plane, and the downstream crab cavity rotates the beam back. In the rest of the rings, both planes stay unaffected.

EIC rings consist of six arcs separated by six straight sections, which are labelled according to the hour markings of a clock from IR2 to IR12. A dedicated IR has been

designed at 6 o'clock, and a potential second IR at 8 o'clock is reserved for future upgrade. To resolve the interference between rings, transfer lines, cooler ERS in IR2, the Electron Storage Ring (ESR) is proposed to be tilted by $\sim 200 \mu\text{rad}$ to avoid vertical bends. Figure 2 illustrates the concept. The

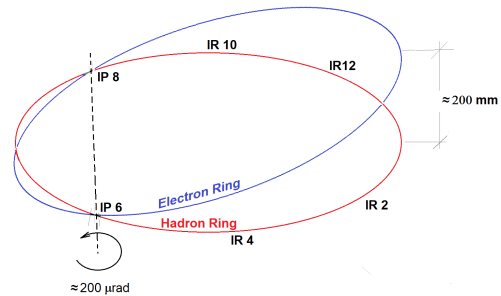


Figure 2: Schematic diagram of tilted ESR in EIC.

rotating axis goes through both interaction points: IP6 and IP8. Although the rotation angle is small, the longitudinal axis is changed, and the dynamic effect has to be studied.

This paper derives the Lorentz Boost formula for the tilted storage rings. The beam-beam simulation is also presented to demonstrate if the tilted scheme works or not. A summary is given at last.

LORENTZ BOOST

When two beams collide with a crossing angle, it is convenient to consider the beam-beam interaction in the boost frame [8], as shown in Fig. 3. Let $(\mathbf{E}_x, \mathbf{E}_y, \mathbf{E}_z)$ be the ba-

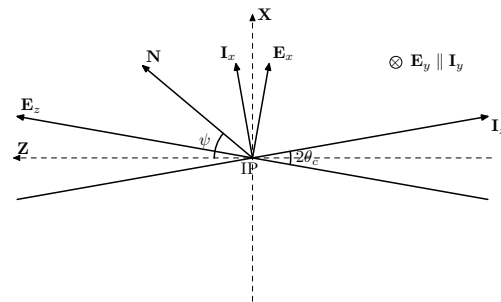


Figure 3: The boost frame for two beams colliding with a large crossing angle. \mathbf{N} points from IP6 to IP8. $\theta_c = 12.5 \text{ mrad}$ is the half crossing angle, and $\psi = \pi/6 + \theta_c$.

sis vectors for the Frenet-Serret frame of the electron ring, and the left-handed $(\mathbf{I}_x, \mathbf{I}_y, \mathbf{I}_z)$ for the ion ring. The vertical axes, \mathbf{E}_y and \mathbf{I}_y , are parallel with each other before rotating the ESR frame. $(\mathbf{X}, \mathbf{Y}, \mathbf{Z})$ are the basis vectors of the boost

* Work supported by Brookhaven Science Associates, LLC under Contract No. DE-SC0012704 with the U.S. Department of Energy
[†] dxu@bnl.gov

frame. In the boost frame,

$$\begin{aligned} \mathbf{N} &= (\sin \psi, 0, \cos \psi)^T, & \mathbf{E}_y &= \mathbf{I}_y = (0, 1, 0)^T \\ \mathbf{E}_z &= (\sin \theta_c, 0, \cos \theta_c)^T, & \mathbf{I}_z &= (\sin \theta_c, 0, -\cos \theta_c)^T \\ \mathbf{E}_x &= (\cos \theta_c, 0, -\sin \theta_c)^T, & \mathbf{I}_x &= (\cos \theta_c, 0, \sin \theta_c)^T \end{aligned} \quad (1)$$

$$R(\mathbf{N}, \phi) = \begin{bmatrix} \cos \phi + (1 - \cos \phi) \sin^2 \psi & -\sin \phi \cos \psi & (1 - \cos \phi) \sin \psi \cos \psi \\ \sin \phi \cos \psi & \cos \phi & -\sin \phi \sin \psi \\ (1 - \cos \phi) \sin \psi \cos \psi & \sin \phi \sin \psi & \cos \phi + (1 - \cos \phi) \cos^2 \psi \end{bmatrix} \quad (2)$$

After the ESR is rotated, the new basis vectors are

$$(\mathbf{E}'_x, \mathbf{E}'_y, \mathbf{E}'_z) = R(\mathbf{E}_x, \mathbf{E}_y, \mathbf{E}_z) \quad (3)$$

$$\mathbf{I}'_x = \mathbf{I}_x, \quad \mathbf{I}'_y = \mathbf{I}_y, \quad \mathbf{I}'_z = \mathbf{I}_z \quad (4)$$

The new crossing angle is determined by their longitudinal axes,

$$\begin{aligned} \cos(2\theta'_c) &= -\mathbf{E}'_z \cdot \mathbf{I}'_z \\ &= \cos(\psi + \theta_c) \cos(\psi - \theta_c) \\ &\quad + \cos \phi \sin(\psi + \theta_c) \sin(\psi - \theta_c) \\ &= \cos(2\theta_c) - (1 - \cos \phi) \sin(\psi + \theta_c) \\ &\quad \times \sin(\psi - \theta_c) \end{aligned} \quad (5)$$

Substituting the numeric value

$$\theta_c = 12.5 \text{ mrad}, \quad \phi = 200 \text{ } \mu\text{rad}, \quad \psi = \pi/6 + \theta_c \quad (6)$$

the new crossing angle is

$$\Delta\theta_c = \theta'_c - \theta_c \approx \frac{\phi^2}{32\theta_c} = 1 \times 10^{-4} \text{ mrad} \quad (7)$$

It turns out the change of the crossing angle is negligible due to the tilted ESR.

The new boost frame is

$$\mathbf{Z}' = \frac{\mathbf{E}'_z - \mathbf{I}'_z}{2 \cos \theta'_c}, \quad \mathbf{X}' = \frac{\mathbf{E}'_z + \mathbf{I}'_z}{2 \sin \theta'_c}, \quad \mathbf{Y}' = \frac{\mathbf{E}'_z \times \mathbf{I}'_z}{\sin(2\theta'_c)} \quad (8)$$

From Eq. (3), Eq. (4), and Eq. (8), \mathbf{E}'_y and \mathbf{I}'_y are no longer parallel with \mathbf{Y}' . To reuse the Hirata map, we need to rotate the vertical axes around their longitudinal axes first. The rotation angles are

$$\begin{aligned} \cos \chi_e &= \mathbf{E}'_y \cdot \mathbf{Y}' \\ &= \frac{-\cos(\psi + \theta_c) \sin(\psi - \theta_c) + \sin(\psi + \theta_c) \cos(\psi - \theta_c) \cos \phi}{\sin(2\theta'_c)} \end{aligned} \quad (9)$$

$$\begin{aligned} \cos \chi_i &= \mathbf{I}'_y \cdot \mathbf{Y}' \\ &= \frac{\sin(\psi + \theta_c) \cos(\psi - \theta_c) - \cos(\psi + \theta_c) \sin(\psi - \theta_c) \cos \phi}{\sin(2\theta'_c)} \end{aligned} \quad (10)$$

Therefore, the new Lorentz Boost map is concatenated by the rotation map and the Hirata map,

$$\mathcal{L}' = \mathcal{R}(\chi) \circ \mathcal{L}(\theta'_c) \quad (11)$$

where θ_c and ψ are defined in Fig. 3, and the superscript "T" denoting the transformation of a vector.

The rotation around \mathbf{N} can be described by a matrix

where \mathcal{R} is a pure rotation around the longitudinal axis, and \mathcal{L} is the well-know Hirata map in [8].

With the numeric values in Eq. (6), the pure rotation angles are

$$\chi_i \approx \chi_e \approx -4 \text{ mrad} \quad (12)$$

which have to be considered in beam-beam simulation.

Due to the rotation in Eq. (12), the $y - z$ coupling is introduced in the boost frame. To prevent the luminosity loss, we have to eliminate the y dependence on z . It can be achieved by introducing the vertical crabbing.

Borrowing the concept from [9], the crab dispersion is defined as

$$\zeta = \left(\frac{\partial x}{\partial z}, \frac{\partial p_x}{\partial z}, \frac{\partial y}{\partial z}, \frac{\partial p_y}{\partial z} \right)^T \quad (13)$$

The crab dispersion caused by the upstream crab cavity is

$$(0, \lambda_x/\Lambda_x, 0, \lambda_y/\Lambda_y)^T$$

where $\Lambda_x = \sqrt{\beta_x^* \beta_{x,c}}$, $\Lambda_y = \sqrt{\beta_y^* \beta_{y,c}}$ are used to normalize the crab cavity strength, $\lambda_{x,y}$ the relative crab cavity kick strength.

Assuming the upstream crab cavity is placed at $\Psi_x = \Psi_y = -\pi/2$ phase advance to IP. After propagated to IP, the crab dispersion turns into

$$\zeta_u = (\lambda_x, 0, \lambda_y, 0)^T \quad (14)$$

Taking the linear term, the Hirata map $\mathcal{L}(\theta'_c)$ is equivalent to a crab dispersion

$$\zeta_L \approx (\theta'_c, 0, 0, 0)^T \quad (15)$$

To provide an effective head-on collision in the boost frame, the crab dispersion in Eq. (14) and Eq. (15) have to cancel with each other,

$$R(\chi) \zeta_u + \zeta_L = 0 \quad (16)$$

where $R(\chi)$ is the 4-by-4 rotation matrix

$$R(\chi) = \begin{bmatrix} \cos \chi & 0 & \sin \chi & 0 \\ 0 & \cos \chi & 0 & \sin \chi \\ -\sin \chi & 0 & \cos \chi & 0 \\ 0 & -\sin \chi & 0 & \cos \chi \end{bmatrix} \quad (17)$$

The required crab cavity can then be resolved,

$$\lambda_x = -\theta'_c \cos \chi, \quad \lambda_y = -\theta'_c \sin \chi \quad (18)$$

The strength of the downstream crab cavity can be determined similarly.

BEAM-BEAM SIMULATION

Figure 4 compares the beam distribution in the boost frame. With appropriate vertical crabbing, the y dependence on z in both electron beam and ion beam is removed.

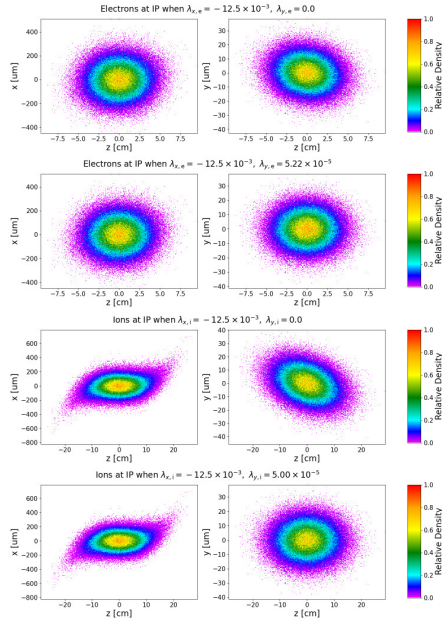


Figure 4: Electron and ion beam distribution in the boost frame.

Figure 5 shows the strong-strong simulation results by BeamBeam3D [10]. With vertical crabbing, the beam size evolution in both ESR and HSR overlaps with the reference curve. Because of the radiation damping and shorter bunch length, the electron beam is still stable even without vertical crabbing. However, when there is no vertical crabbing for the ion ring, the longitudinal motion is coupled to the vertical plane, and the vertical size grows much faster which has to be corrected.

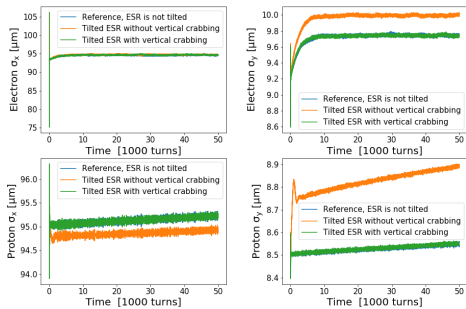


Figure 5: Beam size evolution by strong-strong simulation. The vertical crabbing strength is determined by Eq. (18).

Figure 6 presents the beam size evolution with vertical crabbing only in ion ring. It shows that the tilted ESR is acceptable for the electron beam. The consequence is a slight luminosity loss.

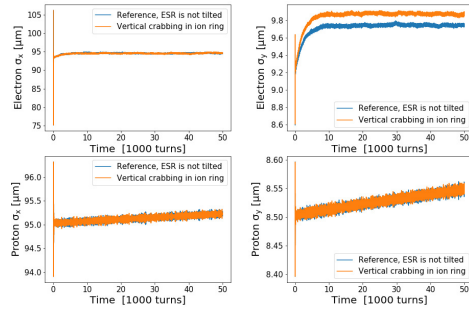


Figure 6: Beam size evolution by strong-strong simulation. Only ion ring is corrected, and there is no vertical crabbing in ESR.

It is well-known that the strong-strong simulation is prone to numeric noise [11]. Therefore, the weak-strong simulation is performed to cross check the vertical crabbing compensation. The similar physical model is used in weak-strong simulation [12], except that the electron beam is assumed as a fixed Gaussian distribution, and the beam-beam kick is calculated by Bassetti-Erskine formula [13].

Figure 7 presents the weak-strong simulation results. Since the vertical plane is problematic, only the vertical size evolution is shown here. EIC adopts the 2nd-order harmonic crab cavity to mitigate the higher-order synchro-betatron resonances [14]. The left plot shows the tracking result without 2nd-order harmonic crab cavity, and the right plot shows the tracking data with 2nd-order harmonic crab cavity. With vertical crabbing and 2nd-order harmonic crab cavity, the vertical growth caused by tilted ESR is compensated. Without vertical crabbing, no matter if 2nd-order harmonic crab cavity is present, the vertical size growth caused by tilted ESR is unacceptable.

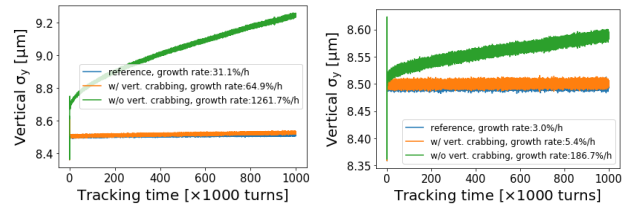


Figure 7: Beam size evolution by weak-strong simulation, left: without 2nd-order harmonic crab cavity, right: with 2nd-order harmonic crab cavity. The last 60% tracking data is fitted with the tracking time $\sigma_y = kt + \sigma_0$, and the growth rate is defined as k/σ_0 .

CONCLUSION

We derived the Lorentz Boost map for the tilted ESR scheme in EIC. The required vertical crabbing strength is calculated to compensate the tilted effect on beam-beam interaction. The strong-strong and weak-strong simulation show that the vertical crabbing is necessary in the ion ring to avoid significant vertical size growth. A realistic scheme to introduce vertical crabbing is described in [15].

REFERENCES

- [1] K. Oide and K. Yokoya, "Beam-beam collision scheme for storage-ring colliders", *Phys. Rev. A*, vol. 40, p. 315, 1989.
- [2] K. Oide *et al.*, "Compensation of the Crossing Angle with Crab Cavities at KEKB", in *Proc. PAC'07*, Albuquerque, NM, USA, Jun. 2007, paper MOZAKI01, pp. 27–31.
- [3] R. Calaga *et al.*, "First demonstration of the use of crab cavities on hadron beams", *Phys. Rev. Accel Beams*, vol. 24.6, p. 062001, 2021.
- [4] Y.-P. Sun *et al.*, "Beam dynamics aspects of crab cavities in the CERN Large Hadron Collider", *Phys. Rev. Spec. Top. Accel Beams*, vol. 12.10, p. 101002, 2009.
- [5] K. Ohmi *et al.*, "Response of colliding beam-beam system to harmonic excitation due to crab-cavity rf phase modulation", *Phys. Rev. Spec. Top. Accel Beams*, vol. 14, p. 111003, 2011.
- [6] D. Xu *et al.*, "Synchrotron resonance of crab crossing scheme with large crossing angle and finite bunch length", *Phys. Rev. Spec. Top. Accel Beams*, vol. 24, p. 041002, 2021.
- [7] F. Willeke, and J. Beebe-Wang, "Electron Ion Collider Conceptual Design Report 2021", United States, 2021. doi:10.2172/1765663
- [8] K. Hirata, "Analysis of beam-beam interactions with a large crossing angle", *Phys. Rev. Lett.*, vol. 74, no. 12, p. 2228.
- [9] Yi-Peng Sun *et al.*, "Crab dispersion and its impact on the CERN Large Hadron Collider collimation", *Phys. Rev. Spec. Top. Accel Beams*, vol. 13, p. 031001, 2010.
- [10] J. Qiang *et al.*, "A parallel particle-in-cell model for beam-beam interaction in high energy ring colliders", *J. Comput. Phys.*, vol. 198, p. 278, 2004.
- [11] F. Kesting and G. Franchetti, "Propagation of numerical noise in particle-in-cell tracking", *Phys. Rev. Spec. Top. Accel Beams*, vol. 18, p. 114201, 2015.
- [12] M. Furman *et al.*, "Comparisons of Beam-Beam Simulations", No. LBL-37680; CBP Note-152, 1995.
- [13] M. Bassetti and G. A. Erskine, "Closed expression for the electrical field of a two-dimensional Gaussian charge", *Tech. Rep.*, 1980.
- [14] D. Xu *et al.*, "Study of Harmonic Crab Cavity in EIC Beam-Beam Simulations", No. BNL-222291-2021-COPA. Brookhaven National Lab (BNL), Upton, NY, United States, 2021.
- [15] D. Xu *et al.*, "Detector solenoid compensation in the EIC Electron Storage Ring", presented at the 13th Int. Particle Accelerator Conf. (IPAC'22), Bangkok, Thailand, June 2022, paper WEPOPT050, this conference.